

# Band Structure of the Jahn-Teller Polaron from Quantum Monte Carlo

P. E. Kornilovitch

*Blackett Laboratory, Imperial College, Prince Consort Road, London SW7 2BZ, UK*

*\*Hewlett-Packard Laboratories, 3500 Deer Creek Road, Palo Alto, California, 94304*

(October 10, 2018)

A path-integral representation is constructed for the Jahn-Teller polaron (JTP). It leads to a perturbation series that can be summed exactly by the diagrammatic Quantum Monte Carlo technique. The ground-state energy, effective mass, spectrum and density of states of the three-dimensional JTP are calculated with no systematic errors. The band structure of JTP interacting with dispersionless phonons, is found to be similar to that of the Holstein polaron. The mass of JTP increases exponentially with the coupling constant. At small phonon frequencies, the spectrum of JTP is flat at large momenta, which leads to a strongly distorted density of states with a massive peak at the top of the band.

PACS numbers: 71.38.+i, 02.70.Lq

The renewed interest in the Jahn-Teller polaron (JTP) problem was sparked by its possible relevance to the colossal magnetoresistance phenomenon in manganese oxides [1–5]. Although cooperative properties of JTPs are of most importance, the solution of the single-JTP problem is a necessary step towards the comprehensive understanding of the physics of these and other materials with Jahn-Teller ions. JTP also bears a significant fundamental interest and it has been a subject of intense theoretical research throughout decades, see, e.g., [6–8]. However, the full quantum-mechanical treatment of this problem is difficult, and no exact solution has been found. Even the single-site JTP does not allow analytical solution. The latter fact has so far prevented the development of a strong-coupling perturbation theory, so successful in the theory of the Holstein polaron [9]. Numerical methods, such as exact diagonalization and density-matrix renormalization group, face the potential difficulty in dealing with a very large Hilbert space of the two phonon modes which are the essential feature of the JTP. Quantum Monte Carlo studies reported so far have treated the phonons only classically [10].

In this paper, a method is presented that allows the full quantum mechanical solution of the JTP problem. The method combines algorithms developed in the Monte Carlo studies of the Holstein [11,12] and Fröhlich [13] polarons. It is based on a path-integral representation of JTP partition function, analytical integration over the phonon coordinates [14,11], and numerical integration over the electron coordinates. The latter is done exactly, with the Diagrammatic Quantum Monte Carlo technique [13]. The use of free boundary conditions in imaginary time [12] allows calculation of the polaron effective mass and the entire spectrum. The method is formulated in continuous time and no systematic errors are introduced. As a result, the ground-state energy, mass, spectrum, and density of states of JTP are calculated exactly on an

finite lattice in the most difficult three-dimensional case. We found that the properties of JTP are very similar to that of the Holstein polaron (HP). JTP is as heavy as HP. It also displays some *anomalous* properties, again similar to HP. In particular, in the case of dispersionless phonons and low phonon frequency, JTP has a flat spectrum at large momenta and a very distorted density of states.

The simplest JTP is an electron that hops between doubly degenerate  $e_g$  levels and interacts locally with a doubly degenerate phonon mode. The model Hamiltonian reads [6]

$$H = H_e + H_{ph} + H_{e-ph}, \quad (1)$$

$$H_e = -t \sum_{\langle \mathbf{n}\mathbf{n}' \rangle} (c_{\mathbf{n}1}^\dagger c_{\mathbf{n}'1} + c_{\mathbf{n}2}^\dagger c_{\mathbf{n}'2}), \quad (2)$$

$$H_{ph} = \sum_{\mathbf{n}} \left[ \frac{1}{2M} (\hat{p}_{x_n}^2 + \hat{p}_{y_n}^2) + \frac{M\omega^2}{2} (x_n^2 + y_n^2) \right], \quad (3)$$

$$H_{e-ph} = -\kappa \sum_{\mathbf{n}} [(c_{\mathbf{n}1}^\dagger c_{\mathbf{n}2} + c_{\mathbf{n}2}^\dagger c_{\mathbf{n}1}) x_n + (c_{\mathbf{n}1}^\dagger c_{\mathbf{n}1} - c_{\mathbf{n}2}^\dagger c_{\mathbf{n}2}) y_n]. \quad (4)$$

Here  $c_{\mathbf{n}a}^\dagger$  creates an electron on site  $\mathbf{n}$  on orbital  $a$  ( $a = 1$  or  $2$  is the orbital index),  $t$  is the intersite hopping matrix element,  $\langle \mathbf{n}\mathbf{n}' \rangle$  denotes pairs of nearest neighbors;  $x_n$  and  $y_n$  are the two phonon displacements on the  $\mathbf{n}$ th site,  $\hat{p}_{x_n, y_n} = -i\hbar\partial_{x_n, y_n}$ ;  $M$  is the ionic mass; and  $\kappa$  is the interaction parameter with dimensionality of force. The energy of the atomic level is set to zero. The model is parameterized by the phonon frequency  $\omega$  and by the dimensionless coupling constant  $\lambda = \kappa^2/(2M\omega^2zt)$  where  $z$  is the number of nearest neighbors. For the simple cubic lattice, considered in this work,  $z = 6$ . Two simplifications are introduced in the model (1)-(4). First, the electron hopping is isotropic, and is diagonal in the orbital index. The latter leads to any change of orbital index taking place only when an  $x$ -phonon is emitted or

absorbed. Averaging over the phonons eliminates all the amplitudes with any odd total number of emission and absorption acts. As a result, the off-diagonal in orbital index elements of the polaron density matrix are identically zero. One can show that such matrix elements determine the splitting between the two polaron bands. The conclusion is that in the model (1)-(4), the two polaron bands are degenerate in the whole Brillouin zone, and there exists only one ground-state dispersion relation  $E_{\mathbf{p}}$ . The second simplification is the absence of the phonon dispersion. It is assumed that each site is surrounded by its own vibrating cluster and the neighboring clusters share no common ions. Such a choice was made to bring the model close to the Holstein model [15]. The difference between the two models lies exclusively in the interaction term (4). This fact will enable us to make a reasonable comparison of JTP and HP. One should add that the full Hamiltonian (1) is invariant under the continuous transformation: rotation in the plane  $(x, y)$  by an angle  $\phi$  (the same for all sites) and simultaneous rotation in the plane  $(c_1, c_2)$  by  $\phi/2$ . The invariance implies the equivalence of the  $x$  and  $y$  modes in the sense that the elastic and interaction energies associated with the two modes must be equal. The number of excited phonons are equal too. These general results serve as independent checks of numerical data.

Central in the proposed method is the path-integral representation for the density matrix  $\rho$  of the model (1)-(4). For a small imaginary-time interval  $\Delta\tau = \beta/L$ , where  $\beta = (k_B T)^{-1}$  is the inverse temperature and  $L \gg 1$ , one obtains, up to the first order in  $\Delta\tau$ :

$$\begin{aligned} \rho(\Delta\tau) &= \langle \mathbf{r}', a'; \{x'_{\mathbf{n}}\}, \{y'_{\mathbf{n}}\} | e^{-\Delta\tau H} | \mathbf{r}, a; \{x_{\mathbf{n}}\}, \{y_{\mathbf{n}}\} \rangle \\ &= [\delta_{\mathbf{r}\mathbf{r}'} \delta_{aa'} + \Delta\tau \kappa \delta_{\mathbf{r}\mathbf{r}'} \delta_{a\bar{a}'} x_{\mathbf{r}} \\ &\quad + \Delta\tau t \delta_{aa'} \sum_{\langle \mathbf{n}\mathbf{n}' \rangle} \delta_{\mathbf{r}, \mathbf{r}'+\mathbf{n}-\mathbf{n}'}] e^{A_{ph}^{\Delta\tau}}, \end{aligned} \quad (5)$$

$$\begin{aligned} A_{ph}^{\Delta\tau} &= \kappa \Delta\tau y_{\mathbf{r}} (\delta_{a1} - \delta_{a2}) \\ &\quad - \sum_{\mathbf{n}} \left\{ \frac{M}{2\hbar^2 (\Delta\tau)} [(x_{\mathbf{n}} - x'_{\mathbf{n}})^2 + (y_{\mathbf{n}} - y'_{\mathbf{n}})^2] \right. \\ &\quad \left. + (\Delta\tau) \frac{M\omega^2}{2} (x_{\mathbf{n}}^2 + y_{\mathbf{n}}^2) \right\}, \end{aligned} \quad (6)$$

$A_{ph}^{\Delta\tau}$  being the phonon action. Here  $\bar{a} = 1, (2)$  when  $a = 2, (1)$ , i.e.  $\bar{a}$  is ‘not’  $a$ . The full density matrix is obtained by multiplying  $\rho(\Delta\tau)$  by itself  $L$  times, introducing integration over the internal coordinates, and taking the  $L \rightarrow \infty$  limit. In doing so, we do *not* impose the periodic boundary conditions in imaginary time but rather leave initial  $\mathbf{r}(0)$ ,  $a(0)$  and final  $\mathbf{r}(\beta)$ ,  $a(\beta)$  coordinates of the electron arbitrary. [Except that  $a(\beta) = a(0)$  always holds.] The boundary conditions on the phonon coordinates are twisted,  $x_{\mathbf{n}}(\beta) = x_{\mathbf{n}-\mathbf{r}(\beta)+\mathbf{r}(0)}(0)$ , and the same for  $y$ , as described in [12]. The next step is to

integrate over  $x_{\mathbf{n}}(\tau)$  and  $y_{\mathbf{n}}(\tau)$ . This is a Gaussian integration and it can be done analytically. Here one faces an important difference between the two phonon modes. Displacements  $y_{\mathbf{n}}(\tau)$  interact with the electron density and do not change the electron coordinates. Therefore, for the oscillators  $y_{\mathbf{n}}$ , the electron is simply a source of external force, the value and sign of which depend on the position and orbital index of the electron, cf. the second term in Eq. (4). The problem reduces to uncoupled oscillators in a time-dependent external field. The integration over  $y_{\mathbf{n}}(\tau)$  can be done by Feynman’s methods [14] to yield the factor  $e^{A_y}$  in the density matrix, where

$$\begin{aligned} &A_y[\mathbf{r}(\tau), a(\tau)] \\ &= \kappa^2 \int_0^\beta \int_0^\beta d\tau d\tau' G(\tau - \tau') [\delta_{a(\tau), a(\tau')} - \delta_{a(\tau), \bar{a}(\tau')}], \end{aligned} \quad (7)$$

$$\begin{aligned} G(\tau - \tau') &= \frac{\hbar}{2M\omega} \left[ e^{-\hbar\omega|\tau-\tau'|} \delta_{\mathbf{r}(\tau), \mathbf{r}(\tau')} \right. \\ &\quad \left. + e^{-\hbar\omega(\beta-|\tau-\tau'|)} \delta_{\mathbf{r}(\tau), \mathbf{r}(\tau')+\text{sign}(\tau-\tau')\Delta\mathbf{r}} \right], \end{aligned} \quad (8)$$

is the retarded action induced by the  $y$  mode. The second term in the function  $G(\tau - \tau')$  involves the net shift of the electron path  $\Delta\mathbf{r} = \mathbf{r}(\beta) - \mathbf{r}(0)$  and the sign of the time difference  $\text{sign}(\tau - \tau') = \pm 1$ , [12]. The simple form (8) of  $G$  is valid in the limit  $e^{\beta\hbar\omega} \gg 1$  that is assumed hereafter. It is important that  $A_y$  is an explicit functional of the electron path and can be calculated straightforwardly once the functions  $\mathbf{r}(\tau)$  and  $a(\tau)$  are specified. Note, that the  $y$ -mode ‘favors’ the same orbital index throughout the whole electron path and ‘dislikes’ orbital changes.

Unlike the  $y$ -mode, the  $x$ -mode changes the orbital index of the electron. It therefore acts like the kinetic energy, but in the ‘orbital space’, compare the last two terms in brackets in Eq.(5). The only complication is that the rate of orbital change is not constant but depends on the local displacement  $x_{\mathbf{r}}(\tau)$ . Nonetheless, the  $x$ -mode and kinetic energy can be treated in the same manner, and this is done as follows. Upon the self-multiplication of  $\rho(\Delta\tau)$ , a variety of terms with different powers of  $(\Delta\tau)$  appear. A term with  $n$  site changes (‘kinks’) and  $m$  orbital changes has the weight

$$\begin{aligned} &(t \Delta\tau)^n (\kappa \Delta\tau)^m x_{\mathbf{r}(\tau_1)}(\tau_1) x_{\mathbf{r}(\tau_2)}(\tau_2) \cdots x_{\mathbf{r}(\tau_m)}(\tau_m) \\ &\quad \times \exp \left\{ - \sum_{\mathbf{n}} \int_0^\beta \left( \frac{M \dot{x}_{\mathbf{n}}^2(\tau)}{2\hbar^2} + \frac{M\omega^2}{2\hbar^2} x_{\mathbf{n}}^2(\tau) \right) d\tau \right\}. \end{aligned} \quad (9)$$

Here  $\tau_s$  is the time of the  $s$ th orbital change ( $s = 1, \dots, m$ ),  $\mathbf{r}(\tau_s)$  is the electron position at this time, and  $x_{\mathbf{r}(\tau_s)}(\tau_s)$  is the  $x$ -displacement at this site at this time. Integration over  $x_{\mathbf{n}}(\tau)$  in (9) can now be performed by introducing fictitious sources, calculating the generating functional and differentiating it  $m$  times. For any odd  $m$  the result is zero, since the  $x$  action is even under the

global sign change  $x_{\mathbf{n}}(\tau) \rightarrow -x_{\mathbf{n}}(\tau)$ . (This is the above-mentioned averaging that leads to the complete degeneracy of the two polaron bands.) For even  $m$ , the time moments  $\tau_s$  should be combined in pairs, and each pair contributes the factor  $\kappa^2 G(\tau_s - \tau_{s'})$  with  $G$  from Eq. (8). Because  $G$  is always positive, the  $x$ -mode ‘favors’ a large number of  $G$ -lines on the electron path, i.e., a large number of orbital changes. Such a tendency is opposite to that of the  $y$ -mode. The competition between the two modes leads to a dynamical balance and to some average number of orbital changes per unit imaginary time. Note also that the same function (8) determines both  $x$  and  $y$  contributions to the density matrix, which reflects the equivalence of the two modes.

Now recall that each term (9) must be still integrated over all the electron positions and orbital indices, i.e., over the time instances of its kinks and orbital changes. Such an integration is denoted below as  $(d\tau)^n$  and  $(d\tau)^m$ . In the  $L \rightarrow \infty$ ,  $\Delta\tau \rightarrow 0$  limit this leads to the path-integral representation of  $\rho$  for JTP:

$$\rho(\beta) = \sum_{n=0,1,\dots}^{\infty} \sum_{m=0,2,\dots}^{\infty} \int_0^{\beta} \dots \int_0^{\beta} (d\tau)^n (d\tau)^m W_{nm}, \quad (10)$$

$$W_{nm} = t^n \kappa^m \left[ \prod_{(\text{pairs of } \tau_s)} G(\tau_s - \tau_{s'}) \right] e^{A_y}. \quad (11)$$

One cannot proceed analytically any further. However, all the integrands are positive-definite, which suggests simulation of  $\rho$  by Monte Carlo (MC) methods. The obvious difficulty is that an *infinite series* of integrals of ever-increasing dimensionality, rather than just one integral, have to be evaluated. Nonetheless the recently developed Diagrammatic MC method [13] is capable of doing such an integration. The method works as follows. Each  $(n, m)$  term in the sum is represented by a diagram (path) with  $n$  kinks and  $m/2$   $G$ -lines, see Fig. 1. The MC process browses the configuration space by means of the two elementary subprocesses: (i) inserting and removing kinks, which changes the dimensionality of integration by 1 ( $n \rightarrow n \pm 1$ ); (ii) attaching and removing  $G$ -lines, which changes the dimensionality by 2 ( $m \rightarrow m \pm 2$ ). The central idea of the method is the balance equation for the two subprocesses [13]. Let  $N_k$  be the number of kinks of a given sort,  $N_k \leq n$ . Next, let  $R(\tau')$  be the normalized probability *density* with which one chooses the position for the new kink. For example, one may decide that all the times in the  $[0, \beta]$  interval are equivalent, hence  $R(\tau') = 1/\beta = \text{const}$ . In the reciprocal removing process, one may decide that any of the  $N_k + 1$  existing kinks are removed with equal probability  $(N_k + 1)^{-1}$ . The resulting balance equation reads:

$$\frac{1}{\beta} W_{nm} P[(n, m) \rightarrow (n + 1, m)] = \frac{1}{N_k + 1} W_{n+1, m} P[(n + 1, m) \rightarrow (n, m)], \quad (12)$$

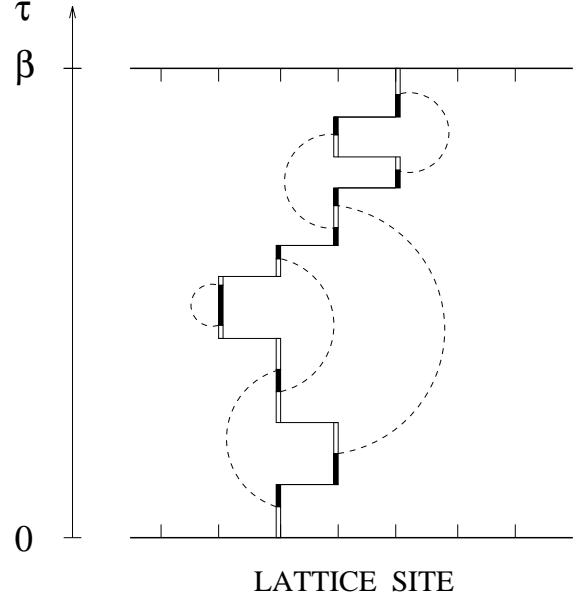


FIG. 1. A typical real space - imaginary time diagram (path) with  $n = 8$  kinks (5 right and 3 left ones, which makes the net shift of the path be  $\Delta\mathbf{r} = 5 - 3 = 2$  lattice sites), and  $m = 12$  orbital changes (6  $G$ -lines). The two different orbital states are shown as black and white segments of the path. Each kink contributes to path’s weight the factor  $t$ , and each pair of orbital changes connected by a dashed line the factor  $\kappa^2 G(\tau' - \tau'')$ . Additionally, there is an overall factor  $e^{A_y}$  induced by the  $y$  phonon mode. Insertion or removal of a kink at time  $\tau'$  shifts the whole segment  $\tau' < \tau \leq \beta$  by one lattice site.  $\Delta\mathbf{r}$  also changes. [Recall that  $\Delta\mathbf{r}$  is an explicit parameter of  $G$ , Eq. (8).] Attaching or removing of a  $G$ -line at times  $\tau', \tau''$  changes the orbital index (‘color’) of the path at  $\tau' < \tau < \tau''$ . This affects the action  $A_y$ , Eq. (7).

from where the acceptance probabilities  $P$  follow in the usual manner [16]. The main feature to note is that the elements of the phase space associated with the two sides of the equation have the *same measure*:  $W_{nm}$  brings  $(d\tau)^{n+m}$ , and  $R(\tau') = 1/\beta$  adds one more  $(d\tau)$  because  $R$  is a probability density. The measure of the right-hand-side is also  $(d\tau)^{n+m+1}$ . That makes both transition probabilities be of the same order, and renders the whole process meaningful. In the case of  $G$ -lines, let  $S(\tau', \tau'')$  be the two-dimensional probability density to attach a new  $G$ -line at times  $\tau'$  and  $\tau''$ . While removing, each of  $N_G + 1$   $G$ -lines may again be chosen with equal probability. The balance equation reads

$$S(\tau', \tau'') W_{nm} P[(n, m) \rightarrow (n, m + 2)] = \frac{1}{N_G + 1} W_{n, m+2} P[(n + 2, m) \rightarrow (n, m)]. \quad (13)$$

Again, the measures of the phase space elements are the same because now  $S$  adds  $(d\tau)^2$ . A possible choice for  $S$

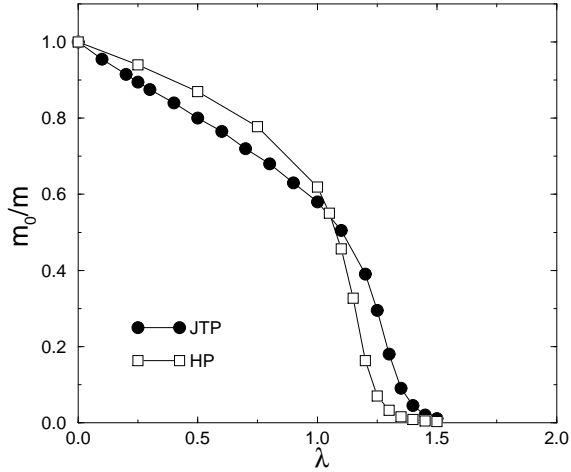


FIG. 2. Inverse effective mass of the three-dimensional JTP (circles) and HP (squares, adopted from [12]) for  $\hbar\omega = 1.0t$ , in units of  $1/m_0 = 2ta_0^2/\hbar^2$ ,  $a_0$  being the lattice constant. Statistical errors are smaller than the symbols.

is  $S(\tau', \tau'') = (\hbar\omega/\beta) \exp(-\hbar\omega|\tau' - \tau''|)$ . The MC process that follows the rules (12)-(13) generates a Markov chain of paths distributed in accordance with Eq.(11). On such an ensemble various polaron properties can be measured with the standard Metropolis rules [16].

One physical quantity that can be calculated with this method is the ground state energy of the polaron  $E_0 = \langle -W_{nm}^{-1}(\partial W_{nm}/\partial\beta) \rangle$  [11,12]. Here we present MC data for two other properties: the effective mass and density of states (DOS). The mass is calculated as the diffusion coefficient of the polaron path,  $m_x^{-1} = (\beta\hbar^2)^{-1}\langle(\Delta r)_x^2\rangle$ , [12]. The inverse mass of the three-dimensional JTP is shown in Fig. 2. After the initial weak-coupling growth  $m/m_0 = 1 + \text{const} \cdot \lambda$ , a transition to the small polaron state takes place at  $\lambda \simeq 1.1 - 1.3$ , and after that the mass increases exponentially with coupling. The comparison with the Holstein polaron (HP) shows that both masses behave similarly. The polaron spectrum is calculated with the formula  $E_{\mathbf{P}} - E_0 = -\beta^{-1} \ln\langle \cos \mathbf{P} \Delta \mathbf{r} \rangle$ , [12], and DOS is obtained by integrating  $E_{\mathbf{P}}$  over the Brillouin zone. The resulting DOS appears to be strongly distorted in the adiabatic regime,  $\hbar\omega = 1.0t$ , see Fig. 3. The polaron spectrum is flat in the outer part of the Brillouin zone due to hybridization with dispersionless phonon modes [17], which results in a massive peak in DOS at the top of the band. The van Hove singularities are invisible because they are absorbed by the peak. All these features are very similar to that of the Holstein polaron [12]. The similarity suggests that such peculiar features of the band structure are common to polaron models with local interaction and dispersionless phonons in the adiabatic regime.

In conclusion, we have developed a path-integral rep-

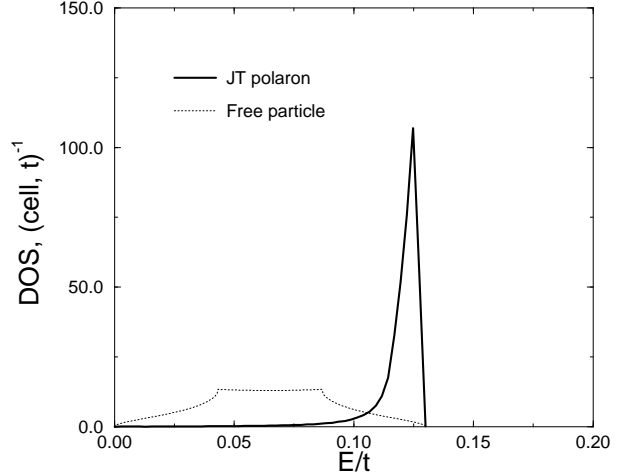


FIG. 3. Density of states of the three-dimensional JTP for  $\hbar\omega = 1.0t$  and  $\lambda = 1.3$ . The polaron bandwidth is  $W = 0.130(5)t$ . The dotted line shows the free-particle DOS with the same  $W$ .

resentation for the Jahn-Teller polaron and used the Diagrammatic Monte Carlo method to simulate the series expansion for its density matrix. The ground state energy, effective mass, spectrum, and density of states have been calculated with no systematic errors. JTP has been found to be very similar to the Holstein polaron and, therefore, to possess some anomalous properties, in particular a strong distortion of the density of states in the adiabatic regime,  $\hbar\omega \leq t$ . Such a distortion may be a consequence of the short-range electron phonon interaction and dispersionless phonon modes.

I am very grateful to Victor Kabanov for suggesting this problem and for numerous helpful discussions on the subject. I also benefited from conversations with A. S. Alexandrov, P. B. Allen, A. M. Bratkovsky, W. M. C. Foulkes, and V. Perebeinos. This work was supported by EPSRC, grant GR/L40113, and by the Quantum Structures Research Initiative of Hewlett-Packard Laboratories (Palo Alto).

\* Present address.

- [1] A. J. Millis, P. B. Littlewood, and B. I. Shraiman, Phys. Rev. Lett. **74**, 5144 (1995).
- [2] Guo-meng Zhao *et al.*, Nature **381**, 676 (1996).
- [3] A. S. Alexandrov and A. M. Bratkovsky, Phys. Rev. Lett. **82**, 141 (1999).
- [4] P. B. Allen and V. Perebeinos, Phys. Rev. B **60**, 10747 (1999).
- [5] L. Vasiliu-Doloc *et al.*, Phys. Rev. Lett. **83** (1999) (to be

published).

- [6] J. Kanamori, J. Appl. Phys. (Suppl.) **31**, S14 (1960).
- [7] A. Abragam and B. Bleaney, *Electron paramagnetic resonance of transition ions* (Clarendon Press, 1970).
- [8] K. I. Kugel and D. I. Khomskii, Usp. Fiz. Nauk **136**, 621 (1982) [Sov. Phys. Usp. **25**, 231 (1982)].
- [9] I. G. Lang and Yu. A. Firsov, Zh. Eksp. Teor. Fiz. **43**, 1843 (1962), [Sov. Phys. JETP **16**, 1301 (1963)]; A. A. Gogolin, Phys. Stat. Sol. B **109**, 95 (1982). A. S. Alexandrov, Phys. Rev. B **46**, 2838 (1992).
- [10] S. Yunoki, A. Moreo, and E. Dagotto, Phys. Rev. Lett. **81**, 5612 (1998); S. Yunoki, T. Hotta, and E. Dagotto, cond-mat/9909254; Y. Motome and M. Imada, J. Phys. Soc. Japan **68**, 16 (1999).
- [11] H. De Raedt and A. Lagendijk, Phys. Rev. Lett. **49**, 1522 (1982); Phys. Rev. B **27**, 6097 (1983).
- [12] P. E. Kornilovitch, Phys. Rev. Lett. **81**, 5182 (1998); Phys. Rev. B **60**, 3237 (1999).
- [13] N. V. Prokof'ev and B. V. Svistunov, Phys. Rev. Lett. **81**, 2514 (1998); N. V. Prokof'ev, B. V. Svistunov, and I. S. Tupitsin, Zh. Eksp. Teor. Fiz. **114**, 570 (1998) [Sov. Phys. JETP **87**, 310 (1998)]; A. S. Mishchenko *et al.*, cond-mat/9910025.
- [14] R. P. Feynman, Phys. Rev. **97**, 660 (1955); *Statistical Mechanics* (Benjamin, Reading, 1972).
- [15] T. Holstein, Ann. Phys. **8**, 325 (1959); *ibid* p. 343.
- [16] N. Metropolis *et al.*, J. Chem. Phys. **21**, 1087 (1953).
- [17] Y. B. Levinson and É. I. Rashba, Rep. Prog. Phys. **36**, 1499 (1973); G. Wellein, H. Röder, and H. Fehske, Phys. Rev. B **53**, 9666 (1996); W. Stephan, Phys. Rev. B **54**, 8981 (1996).